

TECHNICAL NOTE

Suction effects on rockfill compressibility

L. A. OLDECOP* and E. E. ALONSO†

KEYWORDS: constitutive model; oedometer; rockfill; suction

INTRODUCTION

A conceptual mechanism of rockfill deformation was postulated by Oldecop & Alonso (2001) on the basis of the observed rockfill behaviour in suction-controlled oedometer tests. Rockfill mechanical behaviour was linked to water action by means of some crack propagation phenomena, usually known as *subcritical crack growth* (Atkinson, 1984). For most rocks, the propagation velocity of cracks depends on the applied loads and the chemical action of water contained within the rock particles. Water action is conveniently measured by the relative humidity or by the total suction. It is believed that such phenomena are involved in rockfill particle breakage, an experimental fact that is well recognised as being part of rockfill volumetric deformation under a wide range of stress states (Kjaernsli & Sande, 1963; Sowers *et al.*, 1965; Fumagalli, 1969; Marsal, 1973).

A phenomenological constitutive model was proposed (Oldecop & Alonso, 2001) for one-dimensional compression, in which total suction and total stress are the relevant variables. This initial approach was based on a reduced number of laboratory tests, in which the vertical stress was limited to a maximum of 1 MPa. A new experimental programme was performed on the same material, using a newly developed testing device. A large-diameter (300 mm) oedometer, specially designed for the control of relative humidity by means of an air-flow circulation through the specimen, was built. The maximum vertical load was extended to 2.8 MPa in order to investigate the material behaviour in a load range common to rockfill dam structures. New features of rockfill behaviour were observed during this experimental programme. These are described in the paper. Moreover, the previously proposed constitutive model has been reformulated in order to extend its capabilities to cover these new features.

STRESS–STRAIN BEHAVIOUR

Figure 1(a) and (b) shows the paths followed by the tests performed (in a vertical stress – total suction space) and the stress–strain behaviour measured in a compacted crushed slate, 40 mm in maximum particle size. Details of the tested material are given in Oldecop & Alonso (2001). Each test started in an air-dry condition, which means an initial total suction value close to 100 MPa. The vertical stress was increased in steps, allowing the specimen to deform for at least 1000 min under constant stress. Since no steady condi-

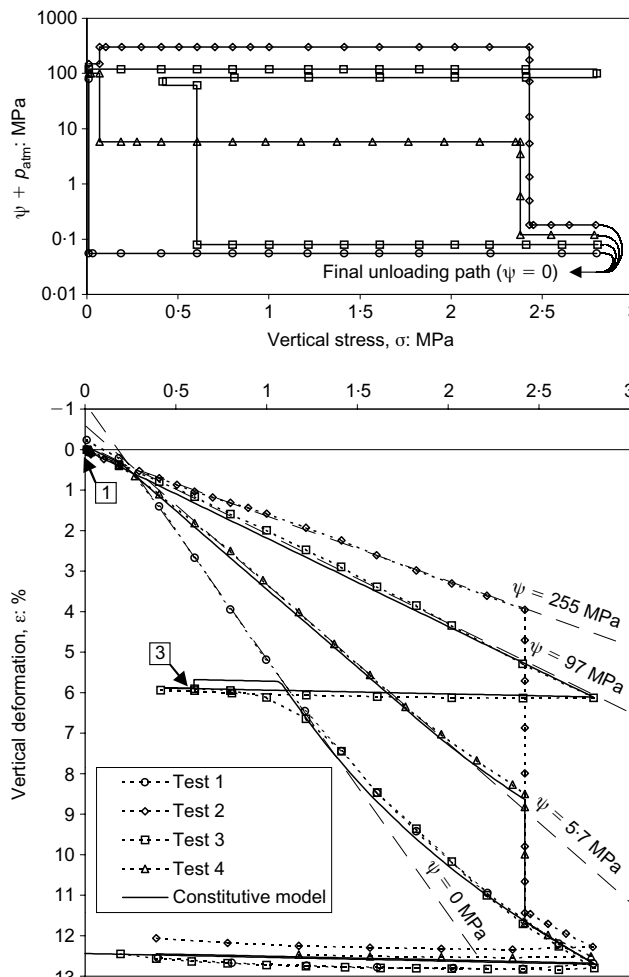


Fig. 1. (a) Loading paths in the stress–suction space followed in the experiments. (b) Vertical stress against measured vertical strain. Square-enclosed numbers indicate the point of flooding of the corresponding specimen. Constitutive model results obtained for stress–suction paths corresponding to tests 3 and 4

tion was attained at any load step (in a strain–log(*t*) type of plot), the strain values used for the stress–strain graphs (Fig. 1(b)) were conventionally defined as the measurement recorded 1000 min after application of the load increment. Total suction changes under constant vertical stress were induced by means of the relative humidity control system (Oldecop & Alonso, 2001), in both the wetting and the drying senses.

The features of rockfill suction-dependent behaviour pointed out in the previous paper are also evident from Fig. 1. As total suction decreases (wetting), the compressibility increases, up to a maximum value corresponding to the saturated state ($\psi = 0$ MPa). Within a wide range of strain values, normal compression lines approach a linear strain–stress relationship. Collapse strains are observed to occur upon wetting under constant vertical load (tests 2 and 4). It

Manuscript received 2 May 2002; revised manuscript accepted 18 November 2002.

Discussion on this paper closes 1 September 2003, for further details see p. ii.

* Earthquake Engineering Institute (IDIA), Universidad Nacional de San Juan, Argentina.

† Department of Geotechnical Engineering and Geosciences, Universitat Politècnica de Catalunya, Barcelona, Spain.

is also clear from Fig. 1(b) that during a short initial stage, under low applied stresses, the described suction-dependent behaviour does not apply, but only beyond a threshold stress value, which will be denoted as σ_y ($\cong 0.20$ MPa). When $\sigma < \sigma_y$, the sole effect of suction changes is the development of rather moderate swelling/shrinkage strains, but no collapse strains occur upon wetting.

The new experimental data, plotted in Fig. 1, extend these early observations. It is shown that the material may attain an even lower compressibility when the specimen is dried beyond the initial 'air-dry' condition (test 2). The formerly postulated uniqueness of normal compression lines (NCL) for each single total suction value seems well supported by the new experiments. Finally, beyond a certain strain value, the stress-strain relationships are no longer linear, but become curved with the concavity directed towards the stress axis: that is, the material stiffens as stress and strain increase. Plotting the same experimental data in a strain-log stress graph (Fig. 2) yields the typical shape of NCLs of granular materials. Isotropic tests performed by Coop & Lee (1995) also showed that NCLs for dry sands lie above those of saturated soils. The present experimental results agree with those early observations and, moreover, suggest that the position of NCLs is controlled by total suction.

Figure 3 shows a plot of strain against total suction data along the collapse paths performed in tests 2 and 4 under constant vertical stress (2.4 MPa). The solid lines are quasi-continuous records of simultaneous readings of strain and suction obtained from an LVDT and a capacitive hygrometer (pairs of data were sampled every 5 min). These records suggest the existence of a direct connection between the collapse phenomenon and total suction.

The type of behaviour shown in Fig. 2 was interpreted in terms of particle breakage mechanisms by a number of authors (Coop & Lee, 1995; Pestana & Whittle, 1995; McDowell & Bolton, 1998). It is widely accepted that during an initial stage, under low applied stresses, deformation occurs as a result only of particle rearrangement. Moreover, it is assumed that the onset of particle breakage leads to the bend in the NCL, causing the rapid increase of the material

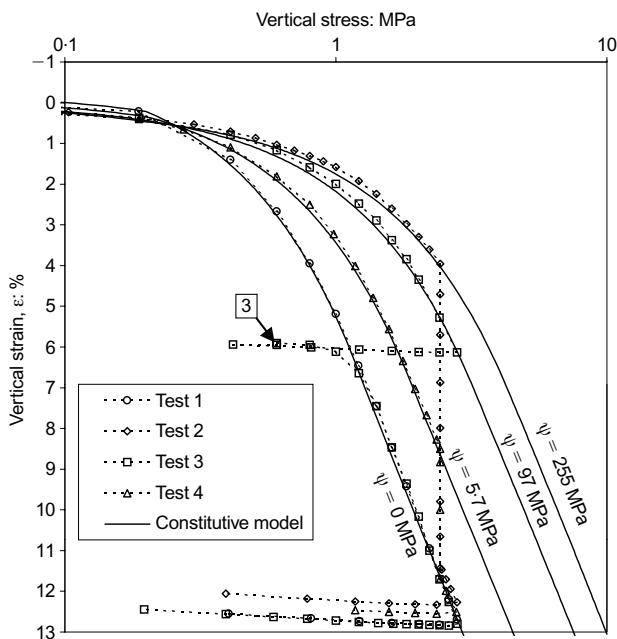


Fig. 2. Experimental results: vertical stress (log scale) against measured vertical strain. Square-enclosed numbers indicate the point of flooding of the corresponding specimen. Model predictions for an extended stress range are also given

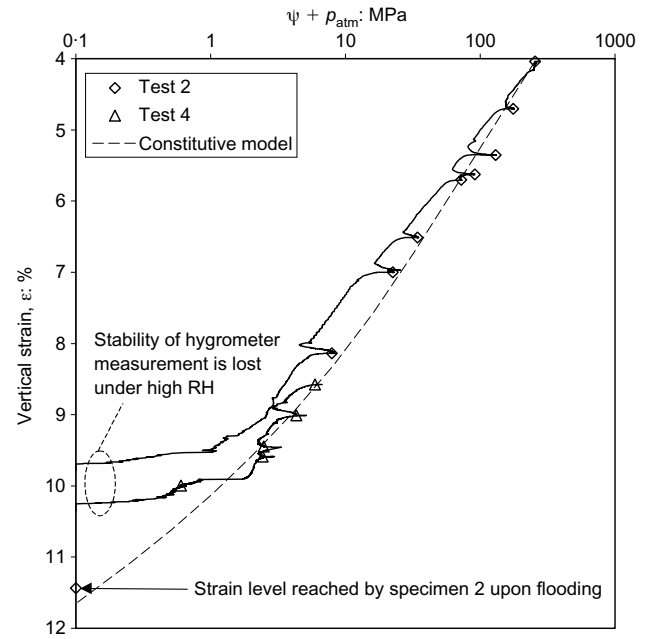


Fig. 3. Strain-suction data obtained along wetting paths performed in tests 2 and 4, under constant vertical stress. Model prediction is also plotted

compressibility index. Under higher loads, the observed linear strain-log stress NCLs were attributed (McDowell & Bolton, 1998) to the particular features of the particle breakage process, when the grain-size distribution approaches a fractal. McDowell & Bolton (1998) called the second and third stages *clastic yielding* and *clastic hardening* respectively. The same nomenclature will be used in the following.

These micromechanical interpretations are in agreement with the present experimental observations, when considered in the framework of the conceptual model proposed by Oldecop & Alonso (2001). The water-dependent features of rockfill mechanical behaviour are supposed to occur as a result of fracture propagation phenomena. Hence such dependence would occur only when particle breakage takes place—that is, during the clastic yielding and clastic hardening stages. As no particle breakage occurs during the particle rearrangement stage, no water dependence should be expected, which is indeed what follows from the experimental data in Figs 1 and 2.

CONSTITUTIVE MODEL

The elasto-plastic constitutive model proposed by Oldecop & Alonso (2001), on the basis of the previous experimental work, is limited to the two first stages of behaviour. In the present paper, the original formulation is extended to the third one.

The particle rearrangement stage ($\sigma_0 < \sigma_y$) is considered separately from the following stages, by means of an independent compressibility index, λ^r , a model parameter. The incremental strain-stress relationship is

$$d\varepsilon = \lambda^r d\sigma_0 \text{ for } \sigma_0 < \sigma_y \tag{1}$$

where $d\varepsilon$ is the total strain increment (elastic plus plastic components) and $d\sigma_0$ is the vertical stress increment. Elastic strain increments may occur as a result of changes in stress or in suction. The following expressions are assumed to give such elastic increments:

$$d\varepsilon^e = \underline{\kappa} d\sigma \quad (2)$$

$$d\varepsilon^\psi = \kappa_\psi \frac{d\psi}{(\psi + p_{\text{atm}})} \quad (3)$$

where κ is the elastic stress-related compressibility index, which is assumed to be independent of water action, κ_ψ is the elastic suction-related swelling/retraction index, which is assumed to be independent of the stress level, and p_{atm} is the atmospheric pressure. Since, during particle rearrangement, suction changes do not produce plastic strains, the yield surface should be a vertical line in the stress–total suction space:

$$F(\sigma, \psi) = \sigma_0 - \sigma_0^* = 0 \text{ for } \sigma_0 < \sigma_y \quad (4)$$

where σ_0^* is the hardening parameter. A physical interpretation of this hardening parameter will arise from the model formulation. The hardening rule becomes

$$d\sigma_0^* = \frac{d\varepsilon^p}{\underline{\lambda}^r - \underline{\kappa}}, \text{ for } \sigma_0^* < \sigma_y \quad (4)$$

During the elastic yielding stage ($\sigma_0^* > \sigma_y$) the compressibility index, λ , should be a function of suction (Fig. 1):

$$d\varepsilon = \underline{\lambda}(\psi) d\sigma_0 \quad (5)$$

The experimental data suggest the following expression for $\lambda(\psi)$:

$$\underline{\lambda}(\psi) = \underline{\lambda}_0 - \alpha_\psi \ln\left(\frac{\psi + p_{\text{atm}}}{p_{\text{atm}}}\right) \quad (6a)$$

and

$$\underline{\lambda}(\psi) \geq \underline{\lambda}^i \quad (6b)$$

where λ_0 , λ^i , and α_ψ are model parameters. λ_0 is the maximum compressibility index corresponding to the saturated material ($\psi = 0$). λ^i has the meaning of a minimum compressibility index. Oldecop & Alonso (2001) hypothesised that a minimum value for the compressibility index would be attained by extreme drying (that is, under a very high suction), calling it the *very dry state*. Such a very dry state could not be reached in the present experimental programme, although a high suction value was imposed on specimen 2 ($\psi = 255$ MPa). However, from a practical point of view the very dry state can be conventionally defined as a high enough suction value, so as to ensure that it will not be exceeded during the loading path considered in the analysis.

The expression for the yield surface and the hardening rule in elastic yielding can be derived as shown, by Oldecop & Alonso (2001):

$$F(\sigma, \psi) = \sigma_0[\underline{\lambda}(\psi) - \underline{\kappa}] - \sigma_y[\underline{\lambda}(\psi) - \underline{\lambda}^i] - \sigma_0^*(\underline{\lambda}^i - \underline{\kappa}) = 0 \quad (7)$$

$$d\sigma_0^* = \frac{d\varepsilon^p}{\underline{\lambda}^i - \underline{\kappa}} \text{ for } \sigma_y < \sigma_0^* < \sigma_0^{\text{ch}} \quad (8)$$

where σ_0^{ch} will be defined shortly.

The experimental data (Figs 1 and 2) suggest that the initiation of the elastic hardening stage is marked by a unique value of plastic strain. This is to be expected, since the type of mechanical behaviour is determined by the actual configuration of the granular structure, and the plastic (volumetric) strain can be considered as a parameter measuring that configuration. Defining a threshold strain value is equivalent to defining a threshold value for the hardening parameter, σ_0^* , in view of equation (8). Hence an additional parameter is introduced, σ_0^{ch} , defined as the value of the hardening parameter that marks the onset of elastic hardening. In order to extend the model into the elastic hardening stage, the yield surface is kept the same as in elastic

yielding (equation (7)) while a new hardening rule is proposed:

$$d\sigma_0^* = \frac{\sigma_0^* - \sigma_y}{\sigma_0^{\text{ch}} - \sigma_y} \frac{d\varepsilon^p}{\underline{\lambda}^i - \underline{\kappa}} \text{ for } \sigma_0^* > \sigma_0^{\text{ch}} \quad (9)$$

The shape of the yield surface in stress–suction space is shown in Fig. 4 for different values of plastic vertical strain.

In the following, a complete set of model parameters is determined on the basis of tests 1 and 2. The very dry state is conventionally defined as the first loading condition of specimen 2 after drying to $\psi^{\text{vd}} = 255$ MPa. The adjustment of linear functions to the normal compression lines in the elastic yielding stage, for the very dry state (test 2) and the saturated state (test 1) respectively, yields the minimum compressibility index, λ^i , and the maximum compressibility index, λ_0 . The first loading steps provide the data for determination of the compressibility index for the particle rearrangement stage, λ^r . The elastic unloading/reloading compressibility index, κ , is computed on the basis of the data obtained during unloading paths. The parameter α_ψ , measuring the variation of the normal compressibility index with suction, is determined by means of equation (6a) for $\psi = \psi^{\text{vd}}$ (then $\lambda(\psi) = \lambda^i$).

The suction-related swelling/retraction index is determined on the basis of the heave strain measured in test 1 upon specimen flooding, taking into account equation (3) and the values $\psi^{\text{ad}} = 97$ MPa, $\Delta\varepsilon_{\text{expansion}} = 0.23\%$ (see Fig. 1).

Finally, the threshold value for the hardening parameter marking the onset of the elastic hardening stage, σ_0^{ch} , is derived from the yield surface equation (equation (7)). This is done by introducing in equation (7) the stress–suction values at the point where the stress–strain relationship departs from the straight line and using the previously computed parameters (λ^i , λ_0 , κ , α_ψ and σ_y). For test 1, as can be seen in Fig. 1, the transition point is attained at $\sigma = 1.20$ MPa and $\psi = 0$ MPa.

The computed model parameters are summarised in Table 1. Once model parameters were identified, tests 3 and 4 were simulated and compared with observed behaviour (Figs 1(b) and 2). NCL lines for an extended stress range were also

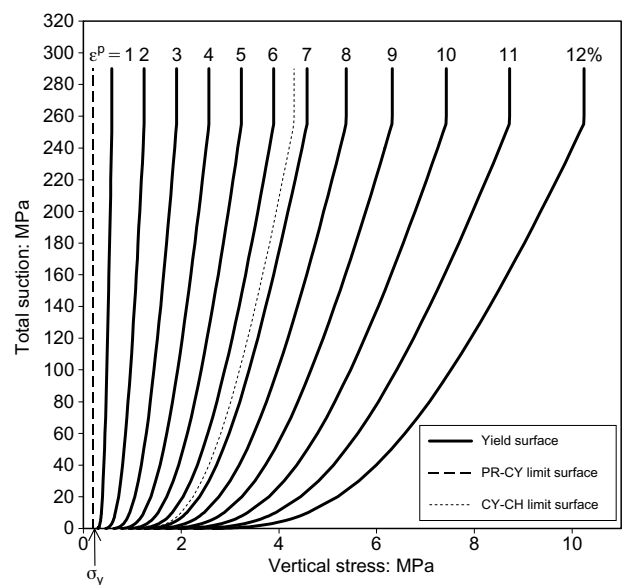


Fig. 4. Yield surfaces corresponding to different plastic strain levels. Limit surfaces are shown between particle rearrangement (PR) and elastic yielding (CY) stages and between elastic yielding and elastic hardening (CH) stages

Table 1. Model parameters determined on the basis of experimental data obtained in tests 1 and 2

λ^r : MPa ⁻¹	2.200×10^{-2}
λ^i : MPa ⁻¹	1.605×10^{-2}
λ_0^d : MPa ⁻¹	6.305×10^{-2}
α_ψ : MPa ⁻¹	0.599×10^{-2}
σ_y : MPa	0.2
κ : MPa ⁻¹	0.092×10^{-2}
κ_ψ : MPa ⁻¹	0.033×10^{-2}
σ_0^{ch} : MPa	4.310

obtained with the model. Computed results are compared in Fig. 2 with the experimental data. In Fig. 3, model results are compared with the strain–suction data collected during collapse paths followed in tests 2 and 4.

CONCLUSIONS

A series of oedometer tests on a rockfill-type material were performed using the relative humidity control technique to investigate the influence of moisture in the mechanical behaviour of the material. The general stress–strain behaviour observed in the experiments is explained in terms of a hardening elasto-plastic material in a generalised stress–suction space.

An extension of a previously proposed elasto-plastic constitutive model is presented in this paper. The model was developed on the basis of one-dimensional compression tests. Total suction is used as the relevant variable measuring the influence of water action on the mechanical behaviour of rockfill. New features included in the present version of the model are related to the ability to correctly reproduce the behaviour in clastic hardening, not taken into account in the initial formulation. The model parameters all have a clear physical meaning and they were determined in a straightforward manner, on the basis of the data obtained in tests 1 and 2. Tests 3 and 4 were reproduced with the model in order to check the ability of the model to reproduce the mechanical behaviour along non-trivial stress–suction paths. The agreement between the model results and the experimental data is very good.

NOTATION

F	yield function
p_{atm}	atmospheric pressure
α_ψ	compressibility parameter

ε	total vertical strain
ε^e	elastic vertical strain due to stress changes
ε^ψ	elastic vertical strain due to suction changes
ε^p	plastic vertical strain
$\Delta\varepsilon_{expansion}$	expansion strain increment due to flooding under zero applied stress
κ	slope of the URL
κ_ψ	suction-based expansion/compression index
λ^r	linear compressibility index in normal compression during particle rearrangement stage
λ	linear compressibility index in normal compression during clastic yielding stage
λ^i	minimum linear compressibility index (very dry state) in clastic yielding
λ_0	maximum linear compressibility index (for $\psi = 0$) in clastic yielding
σ	oedometer vertical stress
σ_y	clastic yield stress (stress threshold that marks the onset of particle breakage)
σ_0	yield vertical stress
σ_0^*	model hardening parameter
σ_0^{ch}	threshold value of σ_0^* marking the onset of the clastic hardening stage
ψ	total suction
ψ^{vd}	total suction in very dry state
ψ^{ad}	total suction in air dry (initial) state

REFERENCES

- Atkinson, B. K. (1984). Subcritical crack growth in geological materials. *J. Geophys. Res.* **89**, No. B6, 4077–4114.
- Coop, M. R. & Lee, I. K. (1995). The influence of pore water on the mechanics of granular soils. *Proc. 11th Eur. Conf. Soil Mech. Found. Engng, Copenhagen* **1**, 1.63–1.72.
- Fumagalli, E. (1969). Tests on cohesionless materials for rockfill dams. *J. Soil Mech. Found. Engng, ASCE* **95**, No. SM1, 313–330.
- Kjaernsli, B. & A. Sande (1963). Compressibility of some coarse-grained materials. *Proc. Wiesbaden Eur. Conf. Soil Mech. Found. Engng* **1**, 245–251.
- Marsal, R. J. (1973). Mechanical properties of rockfill. In *Embankment dam engineering, Casagrande volume* (eds R. C. Hirschfeld and S. J. Poulos). New York: John Wiley & Sons.
- McDowell, G. R. & Bolton, M. D. (1998). On the micromechanics of crushable aggregates. *Géotechnique* **48**, No. 5, 667–679.
- Oldecop, L. A. & Alonso, E. E. (2001) A model for rockfill compressibility. *Géotechnique* **51**, No. 2, 127–139.
- Pestana, J. M. & Whittle, A. J. (1995) Compression model for cohesionless soils. *Géotechnique* **45**, No. 4, 611–631.
- Sowers, G. F., Williams, R. C. & Wallace, T. S. (1965). Compressibility of broken rock and settlement of rockfills. *Proc. 6th Int. Conf. Soil Mech. Found. Engng, Montreal* **2**, 561–565.